Available online at www.sciencedirect.com
ScienceDirect
Journal of Sound and Vibration 314 (2008) 194–216
JOURNAL OF SOUND AND VIBRATION
www.elsevier.com/locate/jsvi

Extended Lindstedt–Poincare method for non-stationary resonances of dynamical systems with cubic nonlinearities

R.R. Pušenjak*

Faculty of Mechanical Engineering, University of Maribor, Smetanova 17, SI-2000 Maribor, Slovenia

Received 31 August 2007; received in revised form 23 November 2007; accepted 2 January 2008
Handling Editor: C. Morfey
Available online 20 February 2008

Abstract

This paper presents the extended Lindstedt–Poincare (EL–P) method, which applies multiple time variables to treat non-stationary oscillations arising in dynamical systems with cubic nonlinearities due to the slowly varied excitation parameters. The method is applied extensively in research of non-stationary vibrations of clamped-hinged beams. Recognizing the aperiodic nature of non-stationary oscillations, the new formulation is presented by adding an additional, slow time scale beside time scales of the nonlinear system, which generally correspond to the incommensurate nonlinear frequencies of the response. Using this concept, a generalized approach of the study to the passage through fundamental, superharmonic and subharmonic resonances is presented in the paper. Effects of slowly varying excitation frequency and slowly varying excitation amplitude on the non-stationary oscillations are studied with the computation of deviations from the stationary response. Although the method is formulated for N-dof dynamical systems having weak cubic nonlinearities, it is applied for non-stationary vibrations, where two-mode shape approximation of damped and undamped clamped-hinged beam, respectively, is used and the simultaneous appearance of internal resonance is taken into account. Stability analysis of stationary solutions is performed and comparisons of stationary resonance curves by results obtained with the incremental harmonic balance (IHB) method show good agreement. The passage through the fundamental resonance of damped and undamped clamped-hinged beam, respectively, is investigated in detail.

1. Introduction

Stationary oscillations of nonlinear dynamical systems are phenomena that seldom appear in practice and can be considered as idealization in the treatment of dynamical systems. Nonlinear oscillations are mostly non-stationary due to the time-varying excitation or control parameters, respectively. Non-stationary oscillations produced by time-varying excitation or control are inherently aperiodic.

Non-stationary responses can be studied analytically for weakly nonlinear dynamical systems only. For this purpose, numerous methods have been asserted in the past. Mitropolski [1] developed the asymptotic method and Agrawal and Ewan-Iwanowski [2] generalized the asymptotic method for treating combination resonance.

*Tel.: +386 2 2207801; fax: +386 2 2207990.
E-mail address: rudi.pusenjak@uni-mb.si

0022-460X/$ - see front matter © 2008 Elsevier Ltd. All rights reserved.
doi:10.1016/j.jsv.2008.01.002

Nayfeh [3] and Nayfeh and Mook [4] developed averaging methods and the method of multiple scales. In the last two decades, the Lindstedt–Poincare method gained much attention. Lau et al. [5] and Chen et al. [6] developed an alternative perturbation procedure of multiple scales for computing aperiodic vibrations and various resonances of N-dof dynamical systems with weak cubic nonlinearities. Although their papers extend applicability of the Lindstedt–Poincare method on computation of aperiodic oscillations, it does not treat non-stationary phenomena at all. Recently, Chen et al. [7] generalized the Lindstedt–Poincare method to multidimensional axially moving systems considering both gyroscopic coefficients and modal damping terms.

The present paper introduces a further generalization of the Lindstedt–Poincare method. In order to conduct analytical studies of non-stationary oscillations arising in N-dof dynamical systems having weak cubic nonlinearities, the extended Lindstedt–Poincare (EL–P) method is generalized by introducing an additional time scale, which corresponds to the slowly varying parameter. This generalization, used by Pušenjak et al. [8], recently is broadened by treating fundamental, superharmonic and subharmonic resonances. By introducing the slow time scale, non-stationary oscillations caused by slowly varying excitation frequency and slowly varying excitation amplitudes, respectively, are analyzed. The paper intends to investigate the phenomenon of non-stationary oscillations and non-stationary resonances of clamped-hinged beam. To be able to understand the deviations from the stationary response, the passages through resonances with different sweep rates are performed. For verification of computed stationary response itself, the incremental harmonic balance (IHB) method, proposed by Pušenjak and Oblak [9], is applied. This method deals with the same type of dynamical systems as presented in this work.

This paper is organized in the following way. In Section 2, the governing system of differential equations is discussed, which describes nonlinear oscillations of damped, multi-degree-of-freedom dynamical systems having cubic nonlinearities. Section 3 contains the formulation of the Lindstedt–Poincare method with multiple time scales for computation of non-stationary oscillations as well as computation of non-stationary fundamental, superharmonic and subharmonic resonances in viscously damped N-dof dynamical systems with cubic nonlinearities. In Section 4 the proposed method is applied to non-stationary oscillations of clamped-hinged beams while simultaneously considering the phenomenon of internal resonance. The cases of fundamental resonances are treated in details. It is shown that superharmonic resonance also appears as the consequence of internal resonance. Section 5 deals with local stability of stationary solutions. Section 6 presents the results of computation of stationary and non-stationary fundamental resonances in both damped and undamped clamped-hinged beam. After an extensive discussion of results, which for the stationary case is compared with results of the IHB method, conclusions and suggestions for future work are drawn in Section 7.

2. Nonlinear oscillation equations of dynamical systems with viscous damping and cubic nonlinearities

Nonlinear oscillations of viscously damped dynamical systems with N-dof and cubic nonlinearities are in general described by the system of differential equations [9]:

$$\sum_{m=1}^{N}\left[M_{nm}\frac{\mathrm{d}^2u_m}{\mathrm{d}t^2}+C_{nm}\frac{\mathrm{d}u_m}{\mathrm{d}t}+K^1_{nm}u_m+\sum_{p=1}^{N}\sum_{q=1}^{N}K^3_{nmpq}u_mu_pu_q\right]=\sum_{h=1}^{M_t}p_{nh}\cos(\omega_ht+\varphi_{nh})\quad(n=1,2,\ldots,N),\quad(1)$$

where u_m $(m=1,2,\ldots,N)$ represent the generalized coordinates as unknowns of the system and first and second derivatives with respect to the time t denote generalized velocities and generalized accelerations, respectively. In mechanical systems, M_{nm}, C_{nm}, K^1_{nm} and $K^3_{N_{nm}}$ are coefficients, which usually mean the mass, damping, linear stiffness and cubic nonlinear stiffness, respectively. Eq. (1) is not limited on such systems only, but can describe electrical, physical, biological, etc., dynamical systems, where appropriate meaning of the coefficients M_{nm}, C_{nm}, K^1_{nm}, $K^3_{N_{nm}}$ is applied. Excitation of Eq. (1) is provided in a multi-tone form, which is composed from M_t harmonic components having in general incommensurate frequencies. Accordingly, p_{nh}, ω_h, φ_{nh} $(h=1,2,\ldots,M_t)$ denote amplitudes, exciting frequencies and eventual phase angles of multi-tone excitation forces (which also may be signals, let us say, in electrical systems). The above formulation is appropriate for the use of the IHB method with multiple time variables in dynamical systems with high cubic nonlinearities. However, the IHB method allows computation of steady-state solutions only. In the present paper, non-stationary responses are treated by means of an alternative perturbation method, which ultimates

that a somewhat restricted class of dynamical systems with small modal damping, natural frequencies of corresponding linear modes, small cubic nonlinearities and single tone harmonic excitation is considered. Nevertheless, for the sake of comparison of steady-state results with the IHB method, it is profitable if the perturbation method is formulated starting from the special dimensionless case of Eq. (1) with

$$M_{nm} = \delta_{nm}, \quad K^1_{nm} = \omega^2_{L_n}\delta_{nm}, \quad \delta_{nm} = \begin{cases} 1, & n = m, \\ 0, & n \neq m, \end{cases} \tag{2}$$

where δ_{nm} denotes Kronecker delta and ω_{L_n} denotes natural frequencies of corresponding linear dinamical system. By introducing small positive expansion parameter ε, coefficients of modal damping as well as coefficients of cubic nonlinearities can be accommodated in the form

$$C_{nm} = \varepsilon c_n \delta_{nm}, \quad K^3_{nmpq} = \varepsilon \Gamma_{nmpq} \tag{3}$$

so that they appear in the same order of ε. Using single tone excitation, $M_t = 1$, which can be simplified by $p_n \cos(\omega t + \varphi_n)$, Eq. (1) becomes:

$$\frac{d^2u_n}{dt^2} + \varepsilon c_n \frac{du_n}{dt} + \omega^2_{L_n} u_n + \varepsilon \sum_{m=1}^{N}\sum_{p=1}^{N}\sum_{q=1}^{N} \Gamma_{nmpq} u_m u_p u_q = p_n \cos(\omega t + \varphi_n), \quad n = 1, 2, \ldots, N. \tag{4}$$

The system is subjected to the harmonic excitation with excitation frequency ω and corresponding phase shifts φ_n. Formulation of the EL–P method provides that excitation amplitudes are expressed as power series of the expansion parameter:

$$p_n = \sum_{k=0}^{\infty} \varepsilon^k p_{nk}, \tag{5}$$

so that Eq. (4) is rewritten in the form

$$\frac{d^2u_n}{dt^2} + \varepsilon c_n \frac{du_n}{dt} + \omega^2_{L_n} u_n + \varepsilon \sum_{m=1}^{N}\sum_{p=1}^{N}\sum_{q=1}^{N} \Gamma_{nmpq} u_m u_p u_q = \sum_{k=0}^{\infty} \varepsilon^k p_{nk} \cos(\omega t + \varphi_n), \quad n = 1, 2, \ldots, N. \tag{6}$$

Using this device, we recognize that amplitudes p_{n1} in Eq. (6) appear at the same order of expansion parameter as modal damping and cubic nonlinearities. Therefore, the treatment of weak excited systems is made possible, when zero-order amplitudes p_{n0} and higher order amplitudes p_{nk} $(k>1)$ are equal to zero. In such circumstances, conditions for appearance of fundamental resonances [4] are fulfilled, which are extensively treated in the present work. Nevertheless, it is worth mentioning that the EL–P method can also be extended in cases of strong excitation by assuming nonzero amplitudes p_{n0}, where all higher order amplitudes p_{nk} $(k>0)$ are equal to zero. If damping in Eq. (6) is neglected, the governing equation of the system with cubic nonlinearities is obtained and treated by Chen and Cheung [10], where the Lindstedt–Poincare method is modified for analysis of a two-degree-of-freedom system with strongly cubic nonlinearities. Particular systems may have some symmetry properties, which can be revealed through relations between coefficients of cubic nonlinearities. For example, coefficients of cubic nonlinearities of a uniform, clamped-hinged beam are related by means of the equation

$$\Gamma_{nmpq} = \Gamma_{mnpq} = \Gamma_{nmqp} = \Gamma_{pqnm}. \tag{7}$$

3. Extended Lindstedt–Poincare method

Extension of the Lindstedt—Poincare method with multiple time scales is based on the paper of Lau et al. [5]. Originally, the method was intended to disseminate the range of computation from periodic to aperiodic oscillations. Because non-stationary oscillations are inherently aperiodic, applicability of the method can be naturally extended on the research of physical phenomena caused by slowly varying parameters. However, the method must be reformulated by adding an additional time scale to describe slowly varying parameters properly. Aperiodic oscillations of the N-dof nonlinear dynamical systems are in general composed of

incommensurate nonlinear frequencies ω_n ($n = 1,2,\ldots,N$), which can be expressed about linear frequencies ω_{n0} of the system by means of power series:

$$\omega_n = \omega_{n0} + \sum_{k=1}^{\infty} \varepsilon^k \omega_{nk} \quad (n = 1, 2, \ldots, N). \tag{8}$$

Eq. (8) in fact means that nonlinearities of the N-dof dynamical system do not affect linear frequencies very much compared to nonlinear frequencies.

Proceeding from Eq. (8), the EL–P method with multiple time scales for the computation of non-stationary oscillations is formulated for fundamental, superharmonic and subharmonic resonance.

3.1. Non-stationary oscillations at fundamental, superharmonic and subharmonic resonances

In order to be able to compute fundamental, superharmonic and subharmonic resonances and furthermore to envisage the possibility of treating combination resonance in future work, it is assumed that the excitation frequency ω can be in general expressed as the combination frequency

$$\omega = \eta \sum_{l=1}^{N} a_l \omega_l. \tag{9}$$

The parameter η denotes the subharmonic factor, which enables that apart from fundamental superharmonic and subharmonic resonances also can be constructed and a_l ($l = 1,2,\ldots,N$) are rational factors in such a way that ηa_l correspond to ratios between excitation frequency and nonlinear frequencies. To specialize the general treatment on the cases of fundamental, superharmonic and subharmonic resonances, it is assumed that excitation frequency ω lies in the vicinity of some weighted linear frequency $\eta\omega_{q0}$ ($1 \leqslant q \leqslant N$) and choose values of rational factors to be equal $a_q = 1$, $a_{l\neq q} = 0$ ($l = 1,2,\ldots,N \wedge l \neq q$). Then, Eq. (9) is rewritten in the form

$$\omega = \eta\omega_q \tag{10}$$

and deviation of the excitation frequency ω from the weighted linear frequency $\eta\omega_{q0}$ can be expressed by means of power series

$$\omega = \eta\left(\omega_{q0} + \sum_{k=1}^{\infty} \varepsilon^k \omega_{qk}\right) = \eta\omega_{q0} + \sum_{k=1}^{\infty} \varepsilon^k \eta\omega_{qk}. \tag{11}$$

To stress the nearness of the excitation frequency ω to the frequency $\eta\omega_{q0}$, the power series (11) for nonlinear frequency ω_q is truncated after the first two terms:

$$\omega \doteq \eta\omega_{q0} + \varepsilon\eta\omega_{q1}, \tag{12}$$

where

$$\sigma = \omega_{q1} \tag{13}$$

is introduced as the detuning parameter. By using the detuning parameter, the excitation frequency ω can be expressed in the form

$$\omega = \eta(\omega_{q0} + \varepsilon\sigma). \tag{14}$$

Formulation of the EL–P method for the computation of non-stationary oscillations at fundamental, superharmonic and subharmonic resonances is therefore based on power series (8) for $N-1$ nonlinear frequencies:

$$\omega_n = \omega_{n0} + \sum_{k=1}^{\infty} \varepsilon^k \omega_{nk} \quad (n = 1, 2, \ldots, N \wedge n \neq q) \tag{15}$$

in addition to Eq. (14) with truncation of the power series (11) for the qth nonlinear frequency to the first two terms. According to Eqs. (14) and (15) we introduce $N+1$ time scales (which sometimes are called time

variables to distinguish between time scales of the EL–P method and time scales $T_n = \varepsilon^n t$ in the standard multiple scales method):

$$\tau_n = \eta\omega_n t \quad (n = 1, 2, \ldots, N \wedge n \neq q), \tag{16a}$$

$$\tau_q = \eta\omega_{q0} t, \tag{16b}$$

$$\tau_{N+1} = \eta\varepsilon t. \tag{16c}$$

The time scale τ_q in Eq. (16b) is a fast time scale and τ_{N+1} in Eq. (16c) is referred to as the slow time scale. Note that the slow time scale τ_{N+1} is distinguished from the time scale $T_1 = \varepsilon t$ in the standard multiple scales method only in subharmonic factor η. This is the reason why independent variables τ_i ($i = 1,\ldots,N+1$) in this paper are simply named time scales. By using time scales, time derivatives $\mathrm{d}/\mathrm{d}t$ and $\mathrm{d}^2/\mathrm{d}t^2$ are replaced by differential operators as follows:

$$\frac{\mathrm{d}}{\mathrm{d}t} = \eta\left(\sum_{i=1, i\neq q}^{N} \omega_i \frac{\partial}{\partial\tau_i} + \omega_{q0}\frac{\partial}{\partial\tau_q} + \varepsilon\frac{\partial}{\partial\tau_{N+1}}\right), \tag{17a}$$

$$\begin{aligned}\frac{\mathrm{d}^2}{\mathrm{d}t^2} = \eta^2\Bigg[&\sum_{i=1, i\neq q}^{N}\sum_{j=1, j\neq q}^{N} \omega_i\omega_j \frac{\partial^2}{\partial\tau_i\partial\tau_j} + \omega_{q0}^2\frac{\partial^2}{\partial\tau_q^2} + \varepsilon^2\frac{\partial^2}{\partial\tau_{N+1}^2} \\ &+ 2\left[\sum_{i=1, i\neq q}^{N} \omega_i\left(\omega_{q0}\frac{\partial^2}{\partial\tau_i\partial\tau_q} + \varepsilon\frac{\partial^2}{\partial\tau_i\partial\tau_{N+1}}\right) + \varepsilon\omega_{q0}\frac{\partial^2}{\partial\tau_q\partial\tau_{N+1}}\right]\Bigg]\end{aligned} \tag{17b}$$

and argument ωt of harmonic excitation in Eq. (6) is expressed in the form:

$$\omega t = \eta(\omega_{q0} + \varepsilon\sigma)t = \tau_q + \sigma\tau_{N+1}. \tag{18}$$

Applying differential operators (17a,b) in place of time derivatives in Eq. (6) and replacing argument of harmonic excitation ωt by Eq. (18), one obtains the following set of nonlinear partial differential equations for $n = 1,2,\ldots,N$:

$$\begin{aligned}&\eta^2\left[\sum_{i=1, i\neq q}^{N}\sum_{j=1, j\neq q}^{N} \omega_i\omega_j\frac{\partial^2 u_n}{\partial\tau_i\partial\tau_j} + \omega_{q0}^2\frac{\partial^2 u_n}{\partial\tau_q^2} + \varepsilon^2\frac{\partial^2 u_n}{\partial\tau_{N+1}^2} + 2\left[\omega_i\left(\omega_{q0}\frac{\partial^2 u_n}{\partial\tau_i\partial\tau_q} + \varepsilon\frac{\partial^2 u_n}{\partial\tau_i\partial\tau_{N+1}}\right)\right.\right. \\ &\quad\left.\left. + \varepsilon\omega_{q0}\frac{\partial^2 u_n}{\partial\tau_q\partial\tau_{N+1}}\right]\right] + \varepsilon c_n\eta\left(\sum_{i=1, i\neq q}^{N} \omega_i\frac{\partial u_n}{\partial\tau_i} + \omega_{q0}\frac{\partial u_n}{\partial\tau_q} + \varepsilon\frac{\partial u_n}{\partial\tau_{N+1}}\right) + \omega_{L_n}^2 u_n + \varepsilon\sum_{m=1}^{N}\sum_{p=1}^{N}\sum_{q=1}^{N}\Gamma_{nmpq}u_m u_p u_q \\ &\quad= \sum_{k=0}^{\infty}\varepsilon^k p_{nk}\cos(\tau_q + \sigma\tau_{N+1} + \varphi_n).\end{aligned} \tag{19}$$

The approximate solution of partial differential Eq. (19) in terms of $N+1$ time scales is sought in the form of the power series:

$$u_n = \sum_{k=0}^{\infty}\varepsilon^k u_{nk}(\tau_1, \tau_2, \ldots, \tau_{N+1}). \tag{20}$$

By placing the assumed solution (20) into Eq. (19) and substituting nonlinear frequencies ω_n by power series (15), Eq. (19) is written as follows:

$$\begin{aligned}
&\eta^2 \sum_{i=1,i\neq q}^{N} \sum_{j=1,j\neq q}^{N} \left(\omega_{i0} + \sum_{k=1}^{\infty} \varepsilon^k \omega_{ik}\right)\left(\omega_{j0} + \sum_{l=1}^{\infty} \varepsilon^l \omega_{jl}\right) \frac{\partial^2\left(\sum_{r=0}^{\infty} \varepsilon^r u_{nr}\right)}{\partial\tau_i \partial\tau_j} + \eta^2 \omega_{q0}^2 \frac{\partial^2\left(\sum_{r=0}^{\infty} \varepsilon^r u_{nr}\right)}{\partial\tau_q^2} \\
&\quad + \eta^2 \varepsilon^2 \frac{\partial^2\left(\sum_{r=0}^{\infty} \varepsilon^r u_{nr}\right)}{\partial\tau_{N+1}^2} + 2\eta^2 \left[\sum_{i=1,i\neq q}^{N} \left(\omega_{i0} + \sum_{k=1}^{\infty} \varepsilon^k \omega_{ik}\right)\left(\omega_{q0} \frac{\partial^2\left(\sum_{r=0}^{\infty} \varepsilon^r u_{nr}\right)}{\partial\tau_i \partial\tau_q} + \varepsilon \frac{\partial^2\left(\sum_{r=0}^{\infty} \varepsilon^r u_{nr}\right)}{\partial\tau_i \partial\tau_{N+1}}\right)\right. \\
&\quad \left. \varepsilon\omega_{q0} \frac{\partial^2\left(\sum_{r=0}^{\infty} \varepsilon^r u_{nr}\right)}{\partial\tau_q \partial\tau_{N+1}}\right] + \varepsilon\eta c_n \left[\sum_{i=1,i\neq q}^{N} \left(\omega_{i0} + \sum_{k=1}^{\infty} \varepsilon^k \omega_{ik}\right) \frac{\partial\left(\sum_{r=0}^{\infty} \varepsilon^r u_{nr}\right)}{\partial\tau_i} + \omega_{q0} \frac{\partial\left(\sum_{r=0}^{\infty} \varepsilon^r u_{nr}\right)}{\partial\tau_q} + \varepsilon \frac{\partial\left(\sum_{r=0}^{\infty} \varepsilon^r u_{nr}\right)}{\partial\tau_{N+1}}\right] \\
&\quad + \omega_{L_n}^2 \left(\sum_{r=0}^{\infty} \varepsilon^r u_{nr}\right) + \varepsilon \sum_{m=1}^{N} \sum_{p=1}^{N} \sum_{q=1}^{N} \Gamma_{nmpq} \left(\sum_{k=0}^{\infty} \varepsilon^k u_{mk}\right)\left(\sum_{l=0}^{\infty} \varepsilon^l u_{pl}\right)\left(\sum_{r=0}^{\infty} \varepsilon^r u_{qr}\right) \\
&= \sum_{k=0}^{\infty} \varepsilon^k p_{nk} \cos(\tau_q + \sigma\tau_{N+1} + \varphi_n). \qquad (21)
\end{aligned}$$

By equating the coefficients of like powers of ε on both sides of Eq. (21) and absorbing terms with respect to indices $q0$ into sums, one obtains a system of linear partial differential equations, which must be solved successively for $n = 1,2,\ldots,N$:

$$\varepsilon^0: \quad \eta^2 \sum_{i=1}^{N} \sum_{j=1}^{N} \omega_{i0}\omega_{j0} \frac{\partial^2 u_{n0}}{\partial\tau_i \partial\tau_j} + \omega_{L_n}^2 u_{n0} = p_{n0} \cos(\tau_q + \sigma\tau_{N+1} + \varphi_n), \qquad (22)$$

$$\begin{aligned}
&\eta^2 \sum_{i=1}^{N} \sum_{j=1}^{N} \omega_{i0}\omega_{j0} \frac{\partial^2 u_{n1}}{\partial\tau_i \partial\tau_j} + \omega_{L_n}^2 u_{n1} = p_{n1} \cos\left(\tau_q + \sigma\tau_{N+1} + \varphi_n\right), \\
\varepsilon^1: \quad &-2\eta^2 \sum_{i=1}^{N} \omega_{i0} \left(\sum_{j=1,j\neq q}^{N} \omega_{j1} \frac{\partial^2 u_{n0}}{\partial\tau_i \partial\tau_j} + \frac{\partial^2 u_{n0}}{\partial\tau_i \partial\tau_{N+1}}\right) - \eta c_n \sum_{i=1}^{N} \omega_{i0} \frac{\partial u_{n0}}{\partial\tau_i} \qquad (23) \\
&- \sum_{m=1}^{N} \sum_{p=1}^{N} \sum_{q=1}^{N} \Gamma_{nmpq} u_{m0} u_{p0} u_{q0},
\end{aligned}$$

$$\begin{aligned}
\varepsilon^2: \quad &\eta^2 \sum_{i=1}^{N} \sum_{j=1}^{N} \omega_{i0}\omega_{j0} \frac{\partial^2 u_{n2}}{\partial\tau_i \partial\tau_j} + \omega_{L_n}^2 u_{n2} = p_{n2} \cos(\tau_q + \sigma\tau_{N+1} + \varphi_n) \\
&-2\eta^2 \left[\sum_{i=1}^{N} \omega_{i0} \left(\sum_{j=1,j\neq q}^{N} \omega_{j1} \frac{\partial^2 u_{n1}}{\partial\tau_i \partial\tau_j} + \frac{\partial^2 u_{n1}}{\partial\tau_i \partial\tau_{N+1}} + \sum_{j=1,j\neq q}^{N} \omega_{j2} \frac{\partial^2 u_{n0}}{\partial\tau_i \partial\tau_j}\right)\right] - \eta^2 \frac{\partial^2 u_{n0}}{\partial\tau_{N+1}^2} \\
&-\eta^2 \left[\sum_{i=1,i\neq q}^{N} \omega_{i1} \left(\sum_{j=1,j\neq q}^{N} \omega_{j1} \frac{\partial^2 u_{n0}}{\partial\tau_i \partial\tau_j} + 2\frac{\partial^2 u_{n0}}{\partial\tau_i \partial\tau_{N+1}}\right)\right] - \eta c_n \left(\sum_{i=1}^{N} \omega_{i0} \frac{\partial u_{n1}}{\partial\tau_i} + \sum_{i=1,i\neq q}^{N} \omega_{i1} \frac{\partial u_{n0}}{\partial\tau_i} + \frac{\partial u_{n0}}{\partial\tau_{N+1}}\right) \qquad (24) \\
&- \sum_{m=1}^{N} \sum_{p=1}^{N} \sum_{q=1}^{N} \Gamma_{nmpq} (u_{m1} u_{p0} u_{q0} + u_{m0} u_{p1} u_{q0} + u_{m0} u_{p0} u_{q1}) \\
&\vdots
\end{aligned}$$

The zero-order partial differential equation (Eq. (22)) is solved by assuming the solution in the form:

$$u_{n0} = A_{n0}(\tau_{N+1}) \cos[\tau_n - \Phi_{n0}(\tau_{N+1})] + E_{n0}(\tau_{N+1}) \cos(\tau_q + \sigma\tau_{N+1} + \varphi_n), \qquad (25)$$

where amplitudes A_{n0} and E_{n0} as well as phase angle Φ_{n0} are modulated in dependence on slow time scale τ_{N+1}. Therefore, solution (25) is essentially aperiodic, which in turn allows non-stationary oscillations to be computed. If the term $A_{n0}(\tau_{N+1})\cos[\tau_n - \Phi_{n0}(\tau_{N+1})]$, which represents a solution of the corresponding homogeneous equation, is substituted into a homogeneous equation, one obtains important relations between

linear frequencies and natural frequencies:

$$\omega_{n0}^2 = \frac{\omega_{L_n}^2}{\eta^2}. \tag{26}$$

On the other hand, particular solution $E_{n0}(\tau_{N+1})\cos(\tau_q + \sigma\tau_{N+1} + \varphi_n)$ itself satisfies Eq. (22). By substituting particular solution into Eq. (22) one obtains the following relation:

$$E_{n0}(\tau_{N+1}) = E_{n0} = \frac{p_{n0}}{(\omega_{L_n}^2 - \eta^2\omega_{q0}^2)} \tag{27}$$

from where it follows amplitudes E_{n0} are coefficients, which are in fact independent of the slow time scale and therefore are not modulated. These coefficients can be computed by Eq. (27) from known excitation amplitudes p_{n0} until $\omega_{L_n}^2 \neq \eta^2\omega_{q0}^2$. When it happens, that $\omega_{L_n}^2 = \eta^2\omega_{q0}^2$, particular solution becomes nonuniform and must be removed from Eq. (25).

The subsequent procedure continues with solving Eq. (23). Solution (25) is substituted into Eq. (23) and the right-hand side of Eq. (23) is examined for secular terms. To assure uniform solution of Eq. (23), secular terms on its right-hand side are removed by fulfilling the corresponding solvability conditions. Considering that secular terms are removed, the general solution of Eq. (23) is constructed. After substitution of the constructed solution into Eq. (23), consideration of solvability conditions and equating like terms on both sides of Eq. (23), unknown coefficients of general solution can be found. When some coefficients cannot be determined at this stage of approximation, they are found in subsequent stages of solving of the set of Eqs. (22)–(24) by repeating the procedure. After all perturbation steps are over, the solution of Eq. (20) can be computed to the desired order of ε.

3.2. Passage through resonance with slowly varying parameters

Non-stationary responses can be obtained in the passage through resonance, if the excitation frequency or excitation amplitude slowly changes with time. The passage through resonance with variable frequency is formulated by means of Eq. (14), where detuning σ becomes a function of the slow time scale τ_{N+1}, $\sigma = \sigma(\tau_{N+1})$. If detuning varies linearly with time, then we have:

$$\sigma = \sigma_0 + r\tau_{N+1}, \tag{28}$$

where σ_0 denotes detuning in the starting time $\tau_{N+1} = 0$ and r denotes the sweep rate or the so-called rate of changing σ.

Alternatively, the presented method can be applied also when the excitation amplitude slowly changes with time. In this case, σ has a fixed value, but one of the excitation amplitudes p_{nk} in Eq. (19) slowly varies with time. Therefore, the selected p_{nk} (with fixed n,k) is in general some function of the slow time scale, $p_{nk} = p_{nk}(\tau_{N+1})$. In a special case, when the excitation amplitude varies linearly with time, we have:

$$p_{nk} = p_{nk}(0) + r\tau_{N+1}, \tag{29}$$

where $p_{nk}(0)$ denotes the value of variable excitation amplitude at the starting time and r denotes the rate of changing excitation amplitude.

4. Non-stationary oscillations of a clamped-hinged beam

The system of nonlinear differential equations (4) can be applied directly for studying the transverse oscillations of a damped clamped-hinged beam. Harmonic excitations can be simplified by taking zero phase shifts. Considering $\varphi_n = 0$ strictly in pertinent equations and using the proper value of η, non-stationary transverse oscillations of the beam are governed by the system of nonlinear partial differential equations (19) for fundamental, superharmonic and subharmonic resonance following the procedure explained in the previous section. In order to treat non-stationary oscillations in detail, it is convenient to study the damped clamped-hinged beam by using the two-mode approximation. For this purpose, analysis of the fundamental resonance of the damped clamped-hinged beam is performed, where Eq. (19) is considered by choosing the

subharmonic factor $\eta = 1$ and by setting the number N of degrees of freedom to be equal to $N = 2$. At fundamental resonance, the beam is subjected to the weak harmonic excitation, which appears in the same order of expansion parameter ε as modal damping and cubic nonlinearities. Therefore, excitation takes the form $\varepsilon p_{n1} \cos \omega t$ at this resonance and the remaining amplitudes p_{n0}, $p_{nk} (k > 1)$ are set equal to zero. On the contrary, in superharmonic and subharmonic resonances, respectively, the excitation amplitude may not be necessarily small [4,11]. In such cases, amplitude p_{n0} in Eq. (19) takes a nonzero value assuring that the excitation force does not appear at the same order of ε as damping and nonlinearities. In this paper, a special case of superharmonic resonance, caused by the influence of internal resonance, is studied. Second natural frequency of the beam ω_{L_2} is approximately three times of the first natural frequency ω_{L_1} so that internal resonances occur simultaneously [4]. It is worth mentioning that in the case of fundamental resonance, linear frequencies are equal to the natural frequencies $\omega_{10} = \omega_{L_1}$ and $\omega_{20} = \omega_{L_2}$, respectively, in Eq. (26). In the sequel, fundamental resonance with the excitation frequency ω near the natural frequency ω_{L_1} is studied in detail.

4.1. Solvability conditions of clamped-hinged beam fundamental resonance with ω near ω_{L_1}

Following the general pattern for the two-mode approximation, non-stationary oscillations in the passage through fundamental resonance of clamped-hinged beam with $\omega \approx \omega_{10} = \omega_{L_1}$ can be computed by the EL–P method by using the following frequencies:

$$\omega = \omega_1 = \omega_{10} + \varepsilon \omega_{11}, \tag{30a}$$

$$\omega_2 = \omega_{20} + \sum_{k=1}^{\infty} \varepsilon^k \omega_{2k}, \tag{30b}$$

where $q = 1$ and the deviation of the excitation frequency ω from the linear frequency ω_{10} is expressed through the detuning parameter σ:

$$\sigma = \omega_{11}, \tag{31}$$

so that the excitation frequency can be written in the form

$$\omega = \omega_{10} + \varepsilon \sigma. \tag{32}$$

By using frequencies, defined through Eqs. (30b) and (32), three time scales are introduced as follows:

$$\tau_1 = \omega_{10} t, \tag{33a}$$

$$\tau_2 = \omega_2 t, \tag{33b}$$

$$\tau_3 = \varepsilon t. \tag{33c}$$

From $q = 1$, $\tau_{N+1} = \tau_3$ it follows that the beam is subjected to the harmonic excitation:

$$\varepsilon p_{n1} \cos(\tau_q + \sigma \tau_{N+1}) = \varepsilon p_{n1} \cos(\tau_1 + \sigma \tau_3). \tag{34}$$

Approximate solution of nonlinear partial differential equations governing non-stationary oscillations in terms of three time scales is sought by means of a power series:

$$u_n = \sum_{k=0}^{\infty} \varepsilon^k u_{nk}(\tau_1, \tau_2, \tau_3). \tag{35}$$

Solutions $u_{nk}(\tau_1,\tau_2,\tau_3)$ of the power series (35) can be computed by solving a system of linear partial differential equations (22)–(24). Using the two-mode approximation, $N = 2$, subharmonic factor $\eta = 1$, time scales (33a–c) and harmonic excitation (34), perturbation steps (22)–(24) recast on the form:

$$\varepsilon^0: \quad \sum_{i=1}^{2} \sum_{j=1}^{2} \omega_{i0} \omega_{j0} \frac{\partial^2 u_{n0}}{\partial \tau_i \partial \tau_j} + \omega_{L_n}^2 u_{n0} = 0\,, \tag{36}$$

$$\varepsilon^1: \quad \sum_{i=1}^{2}\sum_{j=1}^{2}\omega_{i0}\omega_{j0}\frac{\partial^2 u_{n1}}{\partial\tau_i\partial\tau_j}+\omega_{L_n}^2 u_{n1}=p_{n1}\cos(\tau_1+\sigma\tau_3)-2\sum_{i=1}^{2}\omega_{i0}\left(\omega_{21}\frac{\partial^2 u_{n0}}{\partial\tau_i\partial\tau_2}+\frac{\partial^2 u_{n0}}{\partial\tau_i\partial\tau_3}\right)$$
$$-c_n\sum_{i=1}^{2}\omega_{i0}\frac{\partial u_{n0}}{\partial\tau_i}-\sum_{m=1}^{2}\sum_{p=1}^{2}\sum_{q=1}^{2}\Gamma_{nmpq}u_{m0}u_{p0}u_{q0}, \tag{37}$$

$$\varepsilon^2: \quad \sum_{i=1}^{2}\sum_{j=1}^{2}\omega_{i0}\omega_{j0}\frac{\partial^2 u_{n2}}{\partial\tau_i\partial\tau_j}+\omega_{L_n}^2 u_{n2}=-2\sum_{i=1}^{2}\omega_{i0}\left(\omega_{21}\frac{\partial^2 u_{n1}}{\partial\tau_i\partial\tau_2}+\frac{\partial^2 u_{n1}}{\partial\tau_i\partial\tau_3}+\omega_{22}\frac{\partial^2 u_{n0}}{\partial\tau_i\partial\tau_2}\right)$$
$$-\omega_{21}^2\frac{\partial^2 u_{n0}}{\partial\tau_2^2}-2\omega_{21}\frac{\partial^2 u_{n0}}{\partial\tau_2\partial\tau_3}-\frac{\partial^2 u_{n0}}{\partial\tau_3^2}-c_n\left(\sum_{i=1}^{2}\omega_{i0}\frac{\partial u_{n1}}{\partial\tau_i}+\omega_{21}\frac{\partial u_{n0}}{\partial\tau_2}+\frac{\partial u_{n0}}{\partial\tau_3}\right)$$
$$-\sum_{m=1}^{2}\sum_{p=1}^{2}\sum_{q=1}^{2}\Gamma_{nmpq}(u_{m1}u_{p0}u_{q0}+u_{m0}u_{p1}u_{q0}+u_{m0}u_{p0}u_{q1}). \tag{38}$$

$\vdots$

General solution of Eq. (36) has the form

$$u_{n0}=A_{n0}(\tau_3)\cos[\tau_n-\Phi_{n0}(\tau_3)] \quad (n=1,2). \tag{39}$$

Substitution of solution (39) in Eq. (37) gives

$$\sum_{i=1}^{2}\sum_{j=1}^{2}\omega_{i0}\omega_{j0}\frac{\partial^2 u_{n1}}{\partial\tau_i\partial\tau_j}+\omega_{L_n}^2 u_{n1}=p_{n1}\cos(\tau_1+\sigma\tau_3)$$
$$+2\omega_{n0}A_{n0}(\tau_3)\left[\omega_{21}\frac{\mathrm{d}\sin[\tau_n-\Phi_{n0}(\tau_3)]}{\mathrm{d}\tau_2}-\cos[\tau_n-\Phi_{n0}(\tau_3)]\frac{\mathrm{d}\Phi_{n0}(\tau_3)}{\mathrm{d}\tau_3}\right]$$
$$+2\omega_{n0}\frac{\mathrm{d}A_{n0}(\tau_3)}{\mathrm{d}\tau_3}\sin[\tau_n-\Phi_{n0}(\tau_3)]+c_n\omega_{n0}A_{n0}(\tau_3)\sin[\tau_n-\Phi_{n0}(\tau_3)]$$
$$-\frac{1}{4}\sum_{m=1}^{2}\sum_{p=1}^{2}\sum_{q=1}^{2}\Gamma_{nmpq}A_{m0}(\tau_3)A_{p0}(\tau_3)A_{q0}(\tau_3)[\cos[\tau_m+\tau_p+\tau_q-\Phi_{m0}(\tau_3)-\Phi_{p0}(\tau_3)-\Phi_{q0}(\tau_3)]$$
$$+\cos[\tau_m-\tau_p+\tau_q-\Phi_{m0}(\tau_3)+\Phi_{p0}(\tau_3)-\Phi_{q0}(\tau_3)]$$
$$+\cos[\tau_m+\tau_p-\tau_q-\Phi_{m0}(\tau_3)-\Phi_{p0}(\tau_3)+\Phi_{q0}(\tau_3)]$$
$$+\cos[\tau_m-\tau_p-\tau_q-\Phi_{m0}(\tau_3)+\Phi_{p0}(\tau_3)+\Phi_{q0}(\tau_3)]], \tag{40}$$

where

$$\frac{\mathrm{d}sin[\tau_n-\Phi_{n0}(\tau_3)]}{\mathrm{d}\tau_2}=\begin{cases}0, & n=1,\\ \cos[\tau_2-\Phi_{20}(\tau_3)], & n=2.\end{cases} \tag{41}$$

The right-hand side of Eq. (40) contains secular terms, which must be eliminated to obtain a uniform solution. In eliminating secular terms, the phenomenon of the internal resonance is considered simultaneously through relation between nonlinear frequencies:

$$\omega_2=3\omega_1, \tag{42}$$

which can be expressed also by relation between time scales:

$$\tau_2=3(\tau_1+\sigma\tau_3). \tag{43}$$

Secular terms are then eliminated, when terms appearing at $\cos[\tau_1-\Phi_{10}(\tau_3)]$ and $\sin[\tau_1-\Phi_{10}(\tau_3)]$ for $n=1$ and similarly terms appearing at $\cos[\tau_2-\Phi_{20}(\tau_3)]$ and $\sin[\tau_2-\Phi_{20}(\tau_3)]$ for $n=2$, respectively, are

collected together and the obtained expressions are equated by zero. In this manner, one obtains solvability conditions:

$$p_{11}\cos[\sigma\tau_3+\Phi_{10}(\tau_3)]-2\omega_{10}A_{10}(\tau_3)\frac{\mathrm{d}\Phi_{10}(\tau_3)}{\mathrm{d}\tau_3}$$
$$-\frac{1}{4}A_{10}(\tau_3)[\beta_{1111}A_{10}^2(\tau_3)+2\beta_{1212}A_{20}^2(\tau_3)$$
$$+\beta_{1121}A_{10}(\tau_3)A_{20}(\tau_3)\cos[3\sigma\tau_3+3\Phi_{10}(\tau_3)-\Phi_{20}(\tau_3)]]=0, \tag{44}$$

$$-p_{11}\sin[\sigma\tau_3+\Phi_{10}(\tau_3)]+2\omega_{10}\frac{\mathrm{d}A_{10}(\tau_3)}{\mathrm{d}\tau_3}+c_1\omega_{10}A_{10}(\tau_3)+\frac{1}{4}\beta_{1121}A_{10}^2(\tau_3)A_{20}(\tau_3)$$
$$\times\sin[3\sigma\tau_3+3\Phi_{10}(\tau_3)-\Phi_{20}(\tau_3)]=0, \tag{45}$$

$$2\omega_{20}A_{20}(\tau_3)\left[\omega_{21}-\frac{\mathrm{d}\Phi_{20}(\tau_3)}{\mathrm{d}\tau_3}\right]-\frac{1}{4}\left[\frac{1}{3}\beta_{2111}A_{10}^3(\tau_3)\cos[3[\sigma\tau_3+\Phi_{10}(\tau_3)]-\Phi_{20}(\tau_3)]\right.$$
$$\left.+2\beta_{2121}A_{10}^2(\tau_3)A_{20}(\tau_3)+\beta_{2222}A_{20}^3(\tau_3)\right]=0, \tag{46}$$

$$2\omega_{20}\frac{\mathrm{d}A_{20}(\tau_3)}{\mathrm{d}\tau_3}+c_2\omega_{20}A_{20}(\tau_3)-\frac{1}{12}\beta_{2111}A_{10}^3(\tau_3)\sin[3[\sigma\tau_3+\Phi_{10}(\tau_3)]-\Phi_{20}(\tau_3)]=0, \tag{47}$$

where coefficients β_{nmpq} are introduced by means of relation:

$$\beta_{nmpq}=\Gamma_{nmpq}+\Gamma_{nmqp}+\Gamma_{npmq}. \tag{48}$$

By introducing a new variable

$$\gamma(\tau_3)=\sigma\tau_3+\Phi_{10}(\tau_3), \tag{49}$$

Eqs. (44)–(47) can be represented as an autonomous system of nonlinear differential equations, where the slow time scale τ_3 does not appear explicitly:

$$p_{11}\cos(\tau_3)+2\omega_{10}A_{10}(\tau_3)\left[\sigma-\frac{\mathrm{d}\gamma(\tau_3)}{\mathrm{d}\tau_3}\right]-\frac{1}{4}A_{10}(\tau_3)[\beta_{1111}A_{10}^2(\tau_3)+2\beta_{1212}A_{20}^2(\tau_3)$$
$$+\beta_{1121}A_{10}(\tau_3)A_{20}(\tau_3)\cos[3\gamma(\tau_3)-\Phi_{20}(\tau_3)]]=0, \tag{50}$$

$$-p_{11}\sin\gamma(\tau_3)+2\omega_{10}\frac{\mathrm{d}A_{10}(\tau_3)}{\mathrm{d}\tau_3}+c_1\omega_{10}A_{10}(\tau_3)$$
$$+\frac{1}{4}\beta_{1121}A_{10}^2(\tau_3)A_{20}(\tau_3)\sin[3\gamma(\tau_3)-\Phi_{20}(\tau_3)]=0, \tag{51}$$

$$2\omega_{20}A_{20}(\tau_3)\left[\omega_{21}-\frac{\mathrm{d}\Phi_{20}(\tau_3)}{\mathrm{d}\tau_3}\right]-\frac{1}{4}\left[\frac{1}{3}\beta_{2111}A_{10}^3(\tau_3)\cos[3\gamma(\tau_3)-\Phi_{20}(\tau_3)]\right.$$
$$\left.+2\beta_{2121}A_{10}^2(\tau_3)A_{20}(\tau_3)+\beta_{2222}A_{20}^3(\tau_3)\right]=0, \tag{52}$$

$$2\omega_{20}\frac{\mathrm{d}A_{20}(\tau_3)}{\mathrm{d}\tau_3}+c_2\omega_{20}A_{20}(\tau_3)-\frac{1}{12}\beta_{2111}A_{10}^3(\tau_3)\sin[3\gamma(\tau_3)-\Phi_{20}(\tau_3)]=0. \tag{53}$$

Eqs. (50)–(53) represent a system of ordinary nonlinear differential equations, which can be solved by numerous techniques of numerical integration, such as the Runge–Kutta method, to obtain non-stationary oscillations.

4.2. Stationary resonance of a clamped-hinged beam

Stationary resonance curves for fundamental resonance with excitation frequency ω near $\omega_{10}=\omega_{L_1}$ of a clamped-hinged beam with simultaneous internal resonance can be constructed from solvability conditions (50)–(53), where $A_{n0}(\tau_3)=A_{n0}=\text{const}$, $\gamma(\tau_3)=\gamma=\text{const}$ and $\Phi_{20}(\tau_3)=\Phi_{20}=\text{const}$, that is $(\mathrm{d}A_{n0}(\tau_3)/\mathrm{d}\tau_3)=0$, $(\mathrm{d}\gamma(\tau_3)/\mathrm{d}\tau_3)=0$ and $(\mathrm{d}\Phi_{20}(\tau_3)/\mathrm{d}\tau_3)=0$. Eqs. (50)–(53) then become nonlinear algebraic equations involving trigonometric functions:

$$p_{11}\cos\gamma+2\omega_{10}A_{10}\sigma-\frac{1}{4}A_{10}[\beta_{1111}A_{10}^2+2\beta_{1212}A_{20}^2+\beta_{1121}A_{10}A_{20}\cos(3\gamma-\Phi_{20})]=0, \tag{54}$$

$$-p_{11}\sin\gamma+c_1\omega_{10}A_{10}+\frac{1}{4}\beta_{1121}A_{10}^2A_{20}\sin(3\gamma-\Phi_{20})=0, \tag{55}$$

$$2\omega_{20}\omega_{21}A_{20}-\frac{1}{4}\left[\frac{1}{3}\beta_{2111}A_{10}^3\cos(3\gamma-\Phi_{20})+2\beta_{2121}A_{10}^2A_{20}+\beta_{2222}A_{20}^3\right]=0, \tag{56}$$

$$c_2\omega_{20}A_{20}-\frac{1}{12}\beta_{2111}A_{10}^3\sin[3\gamma-\Phi_{20}]=0. \tag{57}$$

By some algebraic manipulations, trigonometric functions can be eliminated giving the system of two polynomial equations:

$$\begin{aligned}&[\beta_{2111}A_{10}^2(\beta_{1111}A_{10}^2+2\beta_{1212}A_{20}^2-8\omega_{10}\sigma)-3\beta_{1121}A_{20}^2(2\beta_{2121}A_{10}^2+\beta_{2222}A_{20}^2-8\omega_{20}\omega_{21})]^2\\&\quad+(4\beta_{2111}c_1\omega_{10}A_{10}^2+12\beta_{1121}c_2\omega_{20}A_{20}^2)^2=16\beta_{2111}^2A_{10}^2p_{11}^2,\end{aligned} \tag{58}$$

$$9A_{20}^2[(2\beta_{2121}A_{10}^2+\beta_{2222}A_{20}^2-8\omega_{20}\omega_{21})^2+16c_2^2\omega_{20}^2]=\beta_{2111}^2A_{10}^6. \tag{59}$$

For an undamped clamped-hinged beam, $c_1=c_2=0$, Eqs. (58) and (59) are simplified to the form

$$\begin{aligned}&\beta_{2111}A_{10}^2(\beta_{1111}A_{10}^2+2\beta_{1212}A_{20}^2-8\omega_{10}\sigma)-3\beta_{1121}A_{20}^2(2\beta_{2121}A_{10}^2\\&\quad+\beta_{2222}A_{20}^2-8\omega_{20}\omega_{21})=\pm4\beta_{2111}A_{10}p_{11},\end{aligned} \tag{60}$$

$$3A_{20}(2\beta_{2121}A_{10}^2+\beta_{2222}A_{20}^2-8\omega_{20}\omega_{21})=\pm\beta_{2111}A_{10}^3. \tag{61}$$

To solve the obtained polynomial equations at the first level of approximation, the excitation frequency ω or detuning σ, respectively, is prescribed. Because the excitation frequency is preferred as a natural parameter, the corresponding detuning is calculated from Eqs. (30a) and (31) as

$$\sigma=\frac{\omega-\omega_{10}}{\varepsilon}. \tag{62}$$

The approximate value of frequency ω_{21} for a given ε can be computed using Eqs. (30a,b) and (42), where only the first two terms of the expansion (30b) are considered:

$$\omega_{21}=\frac{\omega_2-\omega_{20}}{\varepsilon}=\frac{3\omega-\omega_{20}}{\varepsilon}. \tag{63}$$

In fact, by means of the mentioned equations, frequency ω_{21} can be eliminated from polynomial equations (58) and (59) in the damped case or Eqs. (60) and (61) in the undamped case of a clamped-hinged beam. Instead both amplitudes A_{n0} $(n=1,2)$ are computed for a given excitation frequency ω or detuning σ, respectively; the simplest procedure can be applied alternatively. The procedure starts from the known amplitude A_{10} (or A_{20}), then solves Eq. (59) or Eq. (61) for the amplitude A_{20} (or A_{10}) and determines the detuning σ from Eq. (58) or Eq. (60), respectively. It is worth mentioning that polynomial equations can be solved in the case of the undamped clamped-hinged beam by using symbolic computation in Mathematica® 5.2. However, in the damped case numerical procedures such as the Newton–Raphson method must be used. To be able to perform branch tracing, the method must be improved by a suitable continuation method. The arc-length continuation method, proposed in Ref. [9], is implemented and successfully used in computations,

presented in this paper. The unknown frequency ω_{21} can be determined more accurately, when the second level of approximation, based on solving Eq. (38), is considered.

4.3. Passage through fundamental resonance of a clamped-hinged beam

The passage through fundamental resonance of a clamped-hinged beam is conducted with time-varying excitation frequency ω, where the subharmonic factor is set to be equal to $\eta = 1$. As in previous sections, the two-mode approximation is considered with a ratio between the first and the second natural frequency equal to be $\omega_{L_1} : \omega_{L_2} = 1 : 3.2406$ [5]. Due to the strong coupling between both modes, internal resonance appears simultaneously. First, the stationary resonance curve, treated in the previous section is, computed. To determine the effects of the time-varying excitation frequency, Eq. (32) is considered and the detuning parameter is put in the form $\sigma(\tau_3) = \sigma_0 + r\tau_3$, where σ_0 denotes the value of the detuning parameter at the starting time $\tau_3 = 0$ and r means the rate of changing σ. Instead of Eq. (62) with fixed excitation frequency ω, variable detuning in Eq. (50) is computed by means of the following equation:

$$\sigma(\tau_3) = \frac{\omega_0 - \omega_{10}}{\varepsilon} + r\tau_3, \tag{64}$$

where ω_0 denotes the initial value of excitation frequency at starting time $\tau_3 = 0$. For positive values of r, the passage through fundamental resonance is constructed with increasing excitation frequency. The passage through fundamental resonance at decreasing excitation frequency is obtained if the rate of changing σ takes negative values. Besides the excitation frequency ω, frequency ω_{21} in Eq. (52) also varies with time. By combining Eqs. (30b) and (42), the first-order approximation of time-varying frequency ω_{21} takes the following form:

$$\omega_{21} = \frac{3\omega_1 - \omega_{20}}{\varepsilon} = \frac{3\omega_0 - \omega_{20}}{\varepsilon} + 3r\tau_3. \tag{65}$$

After substitution of Eqs. (64) and (65) into the system of autonomous differential equations (50)–(53), numerical integration is performed, giving non-stationary response in the passage through fundamental resonance.

5. Stability analysis

Because differential equations (50)–(53) of fundamental resonance are autonomous, the stability of their solutions can be conveniently determined by means of corresponding linearized equations. Alternatively, stability of the computed solutions can be determined by applying the Floquet theory. The latter method can be used for conducting stability analysis of periodic as well as almost periodic solutions and is presented in Ref. [9]. Because the stability analysis is based on the linearization of differential equations, it is simple to use it in the cases that are considered here and can be briefly outlined in the following.

By using vector notation:

$$\mathbf{w} = \{A_{10}, A_{20}, \gamma, \Phi_{20}\}^{\mathrm{T}}, \quad \mathbf{w}' = \left\{\frac{\mathrm{d}A_{10}}{\mathrm{d}\tau_3}, \frac{\mathrm{d}A_{20}}{\mathrm{d}\tau_3}, \frac{\mathrm{d}\gamma}{\mathrm{d}\tau_3}, \frac{\mathrm{d}\Phi_{10}}{\mathrm{d}\tau_3}\right\}^{\mathrm{T}}, \tag{66}$$

Eqs. (50)–(53) can be rewritten symbolically in the form:

$$\mathbf{w}' = \mathbf{f}(\mathbf{w}), \tag{67}$$

where

$$\mathbf{f}(\mathbf{w}) = \{f_1(\mathbf{w}), f_2(\mathbf{w}), f_3(\mathbf{w}), f_4(\mathbf{w})\}^{\mathrm{T}} \tag{68}$$

and where vector $\mathbf{f}(\mathbf{w})$ is combined from components:

$$f_1 = \frac{4p_{11}\sin\gamma(\tau_3) - 4c_1\omega_{10}A_{10}(\tau_3) - \beta_{1121}A_{10}^2(\tau_3)A_{20}(\tau_3)\sin[3\gamma(\tau_3) - \Phi_{20}(\tau_3)]}{8\omega_{10}}, \tag{69a}$$

$$f_2 = \frac{-12c_2\omega_{20}A_{20}(\tau_3) + \beta_{2111}A_{10}^3(\tau_3)\,\sin[3\gamma(\tau_3) - \Phi_{20}(\tau_3)]}{24\omega_{20}}, \tag{69b}$$

$$f_3 = \frac{4p_{11}\,\cos\,\gamma(\tau_3) + 8\omega_{10}A_{10}(\tau_3)\sigma - A_{10}(\tau_3)[\beta_{1111}A_{10}^2(\tau_3) + 2\beta_{1212}A_{20}^2(\tau_3) + \beta_{1121}A_{10}(\tau_3)A_{20}(\tau_3)\,\cos[3\gamma(\tau_3) - \Phi_{20}(\tau_3)]]}{8\omega_{10}A_{10}(\tau_3)}, \tag{69c}$$

$$f_4 = \frac{24\omega_{20}A_{20}(\tau_3)\omega_{21} - [\beta_{2111}A_{10}^3(\tau_3)\,\cos[3\gamma(\tau_3) - \Phi_{20}(\tau_3)] + 6\beta_{2121}A_{10}^2(\tau_3)A_{20}(\tau_3) + 3\beta_{2222}A_{20}^3(\tau_3)]}{24\omega_{20}A_{20}(\tau_3)}. \tag{69d}$$

Eq. (67) is linearized by using the Jacobian matrix $\mathbf{J}$:

$$\mathbf{w}' = \mathbf{w}_0' + \delta\mathbf{w}' = \mathbf{f}(\mathbf{w}_0) + \left[\frac{\partial f_i}{\partial w_j}\right]_{\mathbf{w}=\mathbf{w}_0} \cdot \delta\mathbf{w} = \mathbf{f}(\mathbf{w}_0) + \mathbf{J}\cdot\delta\mathbf{w} \tag{70}$$

so that a slight perturbation $\delta\mathbf{w}$ of constant solution $\mathbf{w}_0$ satisfies the equation:

$$\delta\mathbf{w}' = \left[\frac{\partial f_i}{\partial w_j}\right]_{\mathbf{w}=\mathbf{w}_0} \cdot \delta\mathbf{w} = \mathbf{J}\cdot\delta\mathbf{w}. \tag{71}$$

Let λ_j $(j = 1,2,\ldots,N)$ represent eigenvalues of the Jacobian matrix or eigenvalues of the equation $\det(\mathbf{J}-\lambda\mathbf{I}) = 0$, respectively. If real parts of eigenvalues $\mathrm{Re}\,(\lambda_j) < 0$ for all j, then the constant solution $\mathbf{w}_0$ is stable and if $\mathrm{Re}\,(\lambda_j) > 0$ for any j, the solution $\mathbf{w}_0$ is unstable. If $\mathrm{Re}\,(\lambda_j) = 0$ for some j and all remaining $\mathrm{Re}\,(\lambda_j) < 0$ $(j \neq k)$, stability of solution $\mathbf{w}_0$ cannot be determined by linearization. This being the case, where nonlinear means must be applied.

6. Results and discussions

For presentation of the EL–P method, passage through fundamental resonance of damped as well as undamped clamped-hinged beam is computed and discussed. In the passage through resonance it is always supposed that starting amplitudes and phases, respectively, are in accordance with amplitudes and phases of stationary response of both increased and decreased excitation frequency. In the present study, internal resonance is considered simultaneously. Non-stationary resonances of both damped and undamped beam are computed for excitation amplitudes $p_{11} = 0.03$ and $p_{21} = 0$, respectively. The two-mode approximation is used, where the ratio between the first and the second natural frequency is equal $\omega_{L_1} : \omega_{L_2} = 1 : 3.2406$. Consequently, the resonance course for variable excitation frequency is computed depending on the dimensionless frequency ratio ω/ω_{L_1}. Due to the fundamental resonance, the subharmonic factor is set to be equal $\eta = 1$. Compared to the results of a computed stationary resonance curve with analysis conducted by Lau et al. [5], who studied only the undamped case, the expansion parameter ε is set to be equal $\varepsilon = 1$. Values of coefficients Γ_{nmpq}, β_{nmpq} can be found elsewhere in the literature [4,10].

6.1. Stationary resonance curves of a clamped-hinged beam

Two types of branches of stationary resonance curves of a clamped-hinged beam exist, which are called in-phase and out-of-phase resonances. Stationary resonance curves of a damped beam with damping coefficients $c_1 = c_2 = 0.001$, which belong to the in-phase and out-of-phase resonances for both oscillation modes, are plotted in Figs. 1 and 2, respectively. In Fig. 1, the amplitude course A_{10} of the first mode of oscillation is shown, where branches of in-phase resonances are denoted as $A_{10}^{\mathrm{in}(1)}$ and $A_{10}^{\mathrm{in}(2)}$ and branches of out-of-phase resonances are denoted as $A_{10}^{\mathrm{out}(1)}$ and $A_{10}^{\mathrm{out}(2)}$, respectively. In Fig. 2, the corresponding amplitude course A_{20} of the second mode of oscillation is plotted, where branches of in-phase resonances are denoted as $A_{20}^{\mathrm{in}(1)}$ and $A_{20}^{\mathrm{in}(2)}$ and branches of out-of-phase resonances are denoted as $A_{20}^{\mathrm{out}(1)}$ and $A_{20}^{\mathrm{out}(2)}$, respectively. In both figures, stable branches are drawn by solid lines and unstable branches are plotted by dotted lines. Different branches of stationary resonance curves, computed by the EL–P method, are compared by results, obtained by the IHB method, which are depicted by broken lines. Branches of solutions in both methods are

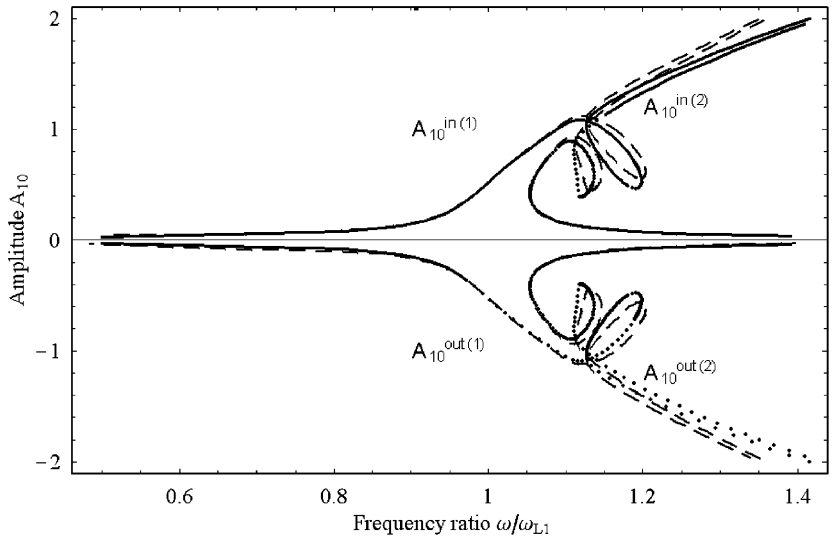

Fig. 1. Stationary resonance of a damped clamped-hinged beam with excitation $p_{11} = 0.03$, $p_{21} = 0$. The course of amplitude A_{10} of the first oscillation mode.

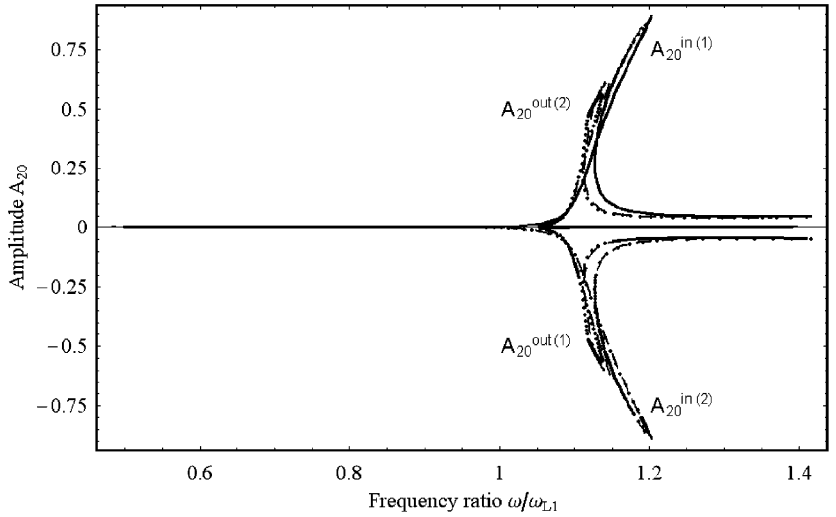

Fig. 2. Stationary resonance of a damped clamped-hinged beam with excitation $p_{11} = 0.03$, $p_{21} = 0$. The course of amplitude A_{20} of the second oscillation mode.

traced by the arc-length continuation method, applied in Ref. [9]. Compared to the results for stationary resonance curves obtained by the EL–P method and the IHB method in Figs. 1 and 2, respectively, it is shown that stationary resonance curves agree reasonable well; however, the EL–P method is much less time consuming. From this observation it is concluded that the EL–P method is reliable and efficient. In the case of amplitude A_{10}, which corresponds to the first oscillation mode of the stationary resonance, in-phase and out-of-phase responses consist of two curves, which for convenience can be denoted as outer and inner curves. Each curve possesses one loop, but a different number of turning points. The outer curve of stationary in-phase and out-of-phase responses has two turning points located on the corresponding loop. The inner curve has three turning points, from which two points are located on the inner curve loop and an extra turning point is placed approximately at the frequency ratio $\omega/\omega_{L_1} = 1.05$, where amplitude A_{10} begins to continually decrease as the frequency increases.

Stationary resonance of the second oscillation mode in Fig. 2 is presented by the course of amplitude A_{20}. Because amplitudes in both in-phase and out-of-phase branches alternatively take positive and negative values, two curves of in-phase and out-of-phase resonances exist. However, they cannot be denoted as inner and outer curve, respectively. Each curve creates one's own loop and possesses turning points. The existence of loops on the resonance curves of both oscillation modes indicates the appearance of superharmonic resonance, which is caused by internal resonance. For given excitation amplitudes $p_{11} = 0.03$, $p_{21} = 0$, superharmonic resonances are present in both in-phase and out-of-phase responses. However, when the excitation amplitude p_{11} increases and reaches a certain critical value, superharmonic resonance disappears. This phenomenon is depicted on branches $A_{10}^{\text{in(2)}}$, $A_{10}^{\text{out(2)}}$ in Fig. 3 for the first mode and on branches $A_{20}^{\text{out(1)}}$, $A_{20}^{\text{out(2)}}$ of Fig. 4 for the

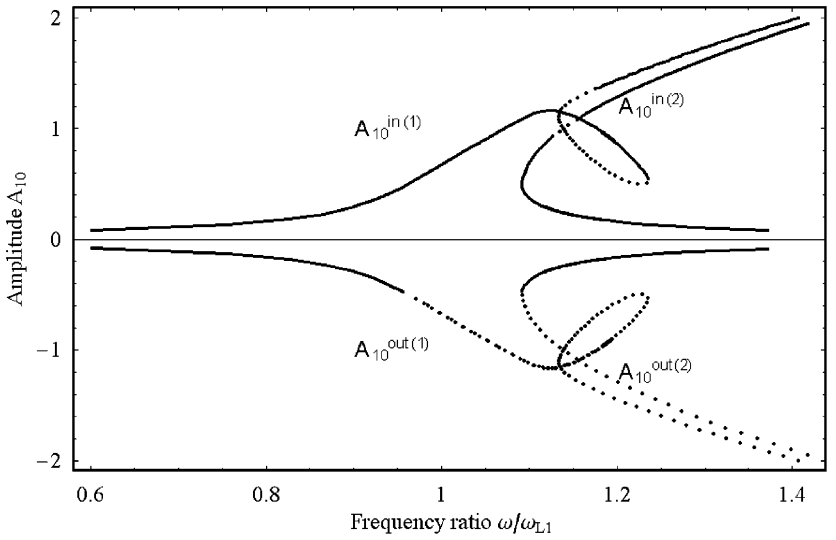

Fig. 3. Stationary resonance of damped clamped-hinged beam with excitation $p_{11} = 0.064$, $p_{21} = 0$: the course of amplitude A_{10} of the first oscillation mode.

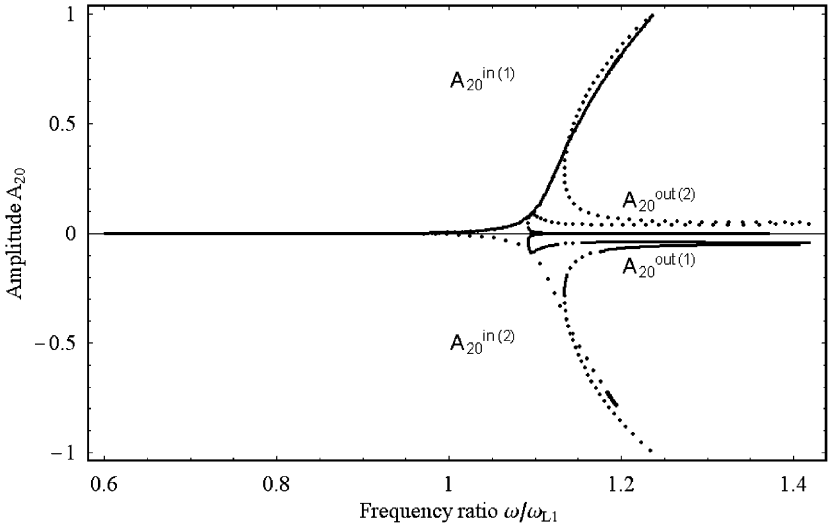

Fig. 4. Stationary resonance of a damped clamped-hinged beam with excitation $p_{11} = 0.064$, $p_{21} = 0$: the course of amplitude A_{20} of the second oscillation mode.

second mode of oscillation. Disappearance of superharmonic resonance at a critical level of excitation due to the internal resonance of the clamped-hinged beam is investigated in details by Chen et al. [6].

6.2. Non-stationary resonance curves of a clamped-hinged beam

To determine the effects of the time-varying excitation frequency, Eq. (32) is considered and a detuning parameter is put into the form $\sigma(\tau_3) = \sigma_0 + r\tau_3$. The examples are first presented for damped and then for the undamped clamped-hinged beam, respectively. Throughout the analysis, the passage through resonance is conducted for positive values of amplitudes only. Because non-stationary response in the passage through resonance is always compared with the stationary one, consequently in-phase and out-of-phase branches of

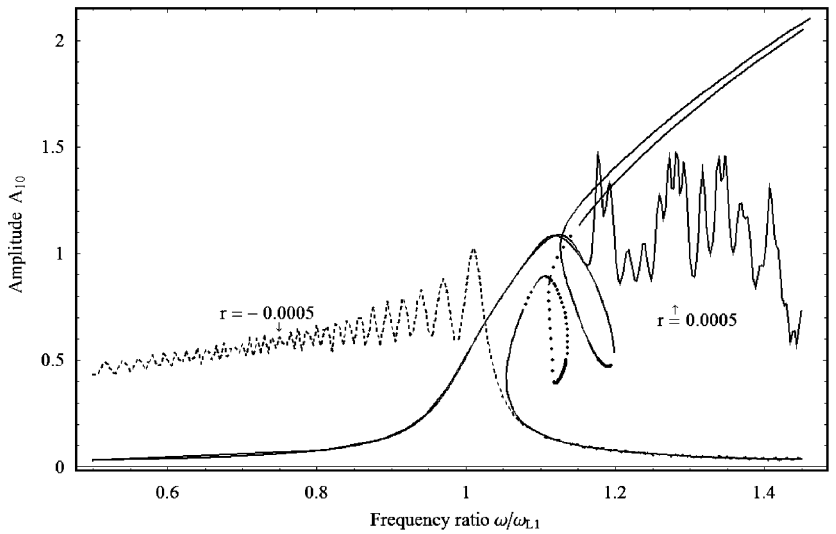

Fig. 5. Passage through fundamental resonance of a damped clamped-hinged beam at small rates of changing σ: the course of amplitude A_{10}.

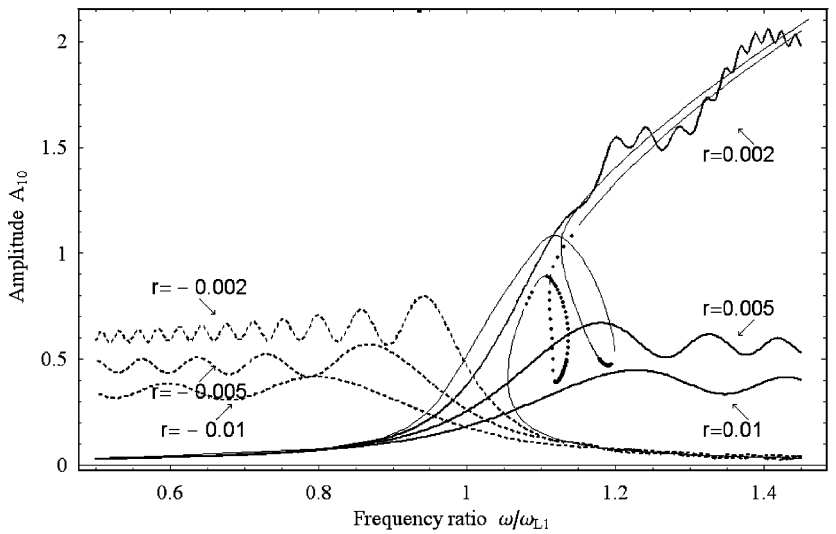

Fig. 6. Passage through fundamental resonance of a damped clamped-hinged beam at greater rates of changing σ: the course of amplitude A_{10}.

stationary resonance curves are shown, having only positive values of amplitudes. The advantage of the EL–P method is that non-stationary responses cannot be computed by the IHB method and therefore comparison of results between the EL–P method and the IHB method in a non-stationary cases is not possible.

The results of computation of non-stationary frequency response of a damped clamped-hinged beam for the first mode of oscillations are presented in Figs. 5 and 6 and for the second mode of oscillations in Figs. 7 and 8, respectively. The non-stationary course of amplitude A_{10} is plotted together with branches of the stationary in-phase resonance course.

The passage through fundamental resonance is conducted for various rates of changing σ, where both increasing and decreasing frequencies are applied. The passage through resonance with increasing frequency begins at the starting frequency ratio $\omega/\omega_{L_1} = 0.5$ and embraces the dimensionless frequency range

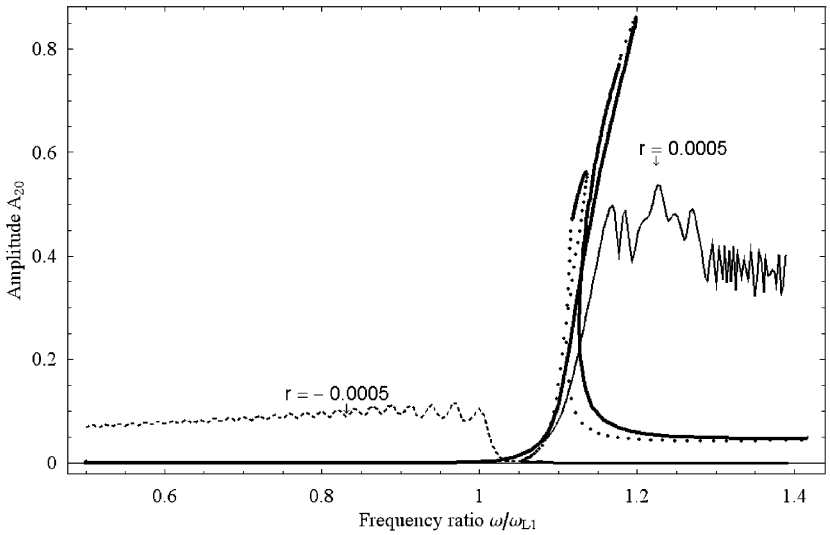

Fig. 7. Passage through fundamental resonance of a damped clamped-hinged beam at small rates of changing σ: the course of amplitude A_{20}.

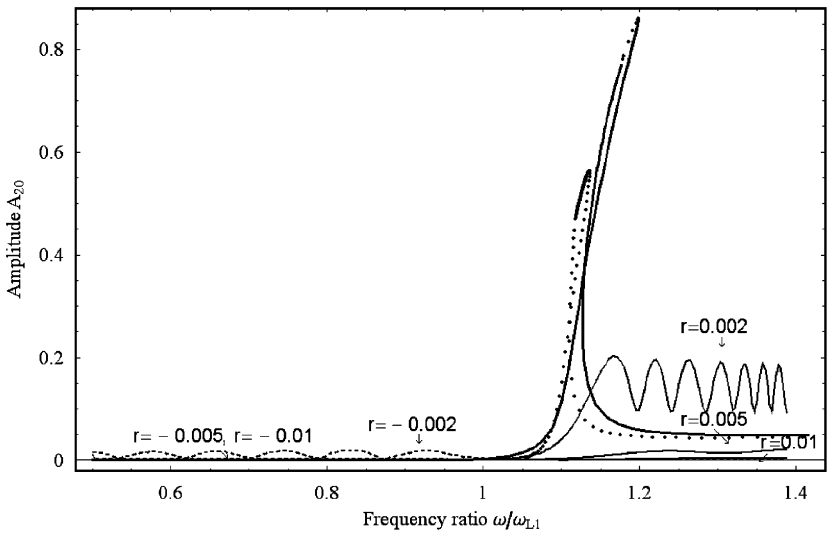

Fig. 8. Passage through fundamental resonance of a damped clamped-hinged beam at greater rates of changing σ: the course of amplitude A_{20}.

$0.5 \leqslant \omega/\omega_{L_1} \leqslant 1.4$. Thereafter, the passage for decreasing frequency is performed in the same range, where frequency takes the starting value, which corresponds to the frequency ratio $\omega/\omega_{L_1} = 1.4$ and then decreases continually. Fig. 5 represents the passage through fundamental resonance at rate $r = \pm 0.0005$ and Fig. 6 shows the corresponding passages through fundamental resonance at rates $r = \pm 0.002$, ± 0.005 and ± 0.01, respectively. For the increased frequency, the non-stationary response of the amplitude A_{10} first follows the stationary response, but sooner or later starts to deviate from it. The smaller the absolute value of rate, later deviations from the stationary curve appear in the passage through resonance. The non-stationary response in the case of the smallest rate $r = 0.0005$ in Fig. 5 first follows the stationary response, next passes the first local maxima and then continues along the stationary curve towards the first turning point on the outer loop and then develops the beat phenomenon.

Passages through fundamental resonance with greater rates $r = 0.002$, 0.005 and 0.01 in Fig. 6 show non-stationary responses, which leave the stationary curve much before the first local maxima and develop the beat phenomenon after the frequency ratio corresponding to the local maxima is exceeded. At rate $r = 0.002$, the beat phenomenon appears, which oscillates around the outer and inner stationary curve with increasing tendency. At rates $r = 0.005$ and 0.01, respectively, the amplitude of local maxima is never reached and the beat phenomenon oscillates with smaller and smaller subsequent peaks as the frequency increases. Frequencies where these peaks appear increase more as the rate of changing σ increases. Non-stationary response of amplitude A_{10} for decreasing frequency with the corresponding negative value of rate is obtained, where the response emanates from branch $A_{10}^{\mathrm{in}(2)}$ on the lowest part of inner stationary curve. Non-stationary response first follows the stationary response by starting at a selected initial frequency and later deviates from the stationary curve as the excitation frequency decreases. Deviations from the stationary curve are more pronounced as the excitation frequency decreases toward the frequency of the third turning point on the inner curve. The maximum peak amplitude and the frequency of the maximum peak decrease as the negative value of rate of changing σ increases. After the maximum peak amplitude is reached, the beat phenomenon develops and the non-stationary resonance curve oscillates with smaller and smaller subsequent peaks as the frequency decreases.

Frequencies, at which these peaks appear are lower if negative rates increase. The smaller the negative rate of changing σ, the more the beat phenomenon is decayed and dies away by approaching towards the stationary response curve. Due to the nonlinearity, asymmetry appears between response curves at increasing and decreasing frequency, respectively. Asymmetry is pronounced more, as the rate of changing σ is smaller.

Figs. 7 and 8 represent the passage through fundamental resonance of the second mode oscillation. In Fig. 7, the excitation frequency increases with the smallest rate ($r = 0.0005$) of changing σ and Fig. 8 shows the passage with increasing excitation frequency at greater rates $r = 0.002$, 0.005 and 0.01. For decreasing excitation frequency, the corresponding negative values of rates are considered. The non-stationary responses with decreasing frequency in both Figs. 7 and 8 emanate from a part of branch $A_{20}^{\mathrm{out}(2)}$ of stationary response, which spreads in the vicinity of the frequency axis (compare to Fig. 2).

It is evident that similar conclusions regarding beat phenomenon evolution also hold in this case. The second mode non-stationary oscillation is more weakly excited as the first mode non-stationary oscillation.

The results of computation of the non-stationary frequency response of the undamped clamped-hinged beam for the first mode of oscillations are presented in Figs. 9 and 10 and for the second mode of oscillations in Figs. 11 and 12, respectively. The non-stationary course of amplitude A_{10} is plotted together with branches of the stationary in-phase resonance course. The passage through fundamental resonance is conducted for various rates of changing σ, where both increasing and decreasing frequencies are applied under equal conditions as in the damped case. Therefore, the passage through resonance with increasing frequency begins at the starting frequency ratio $\omega/\omega_{L_1} = 0.5$ and embraces the dimensionless frequency range $0.5 \leqslant \omega/\omega_{L_1} \leqslant 1.4$. Thereafter, the passage for decreasing frequency is performed in the same range, where frequency takes the starting value, which corresponds to the frequency ratio $\omega/\omega_{L_1} = 1.4$ and then decreases continually. Fig. 9 represents the passage through fundamental resonance at rate $r = \pm 0.0005$, and Fig. 10 shows the corresponding passages through fundamental resonance at rates $r = \pm 0.002$, ± 0.005 and ± 0.01, respectively. Because there is a full correspondence with the damped case, non-stationary responses behave like responses in the damped case at all rates of changing σ. It is proved that damping has great impact on amplitudes as well as on frequencies of peaks in the beat phenomenon at small rates r (compare Figs. 5 and 9) and small impact at

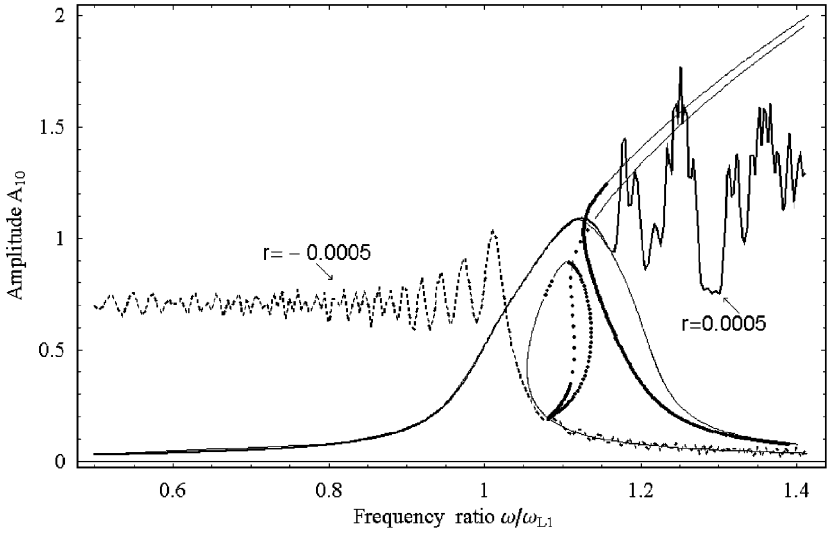

Fig. 9. Passage through fundamental resonance of an undamped clamped–hinged beam at small rate of changing σ: the course of amplitude is A_{10}.

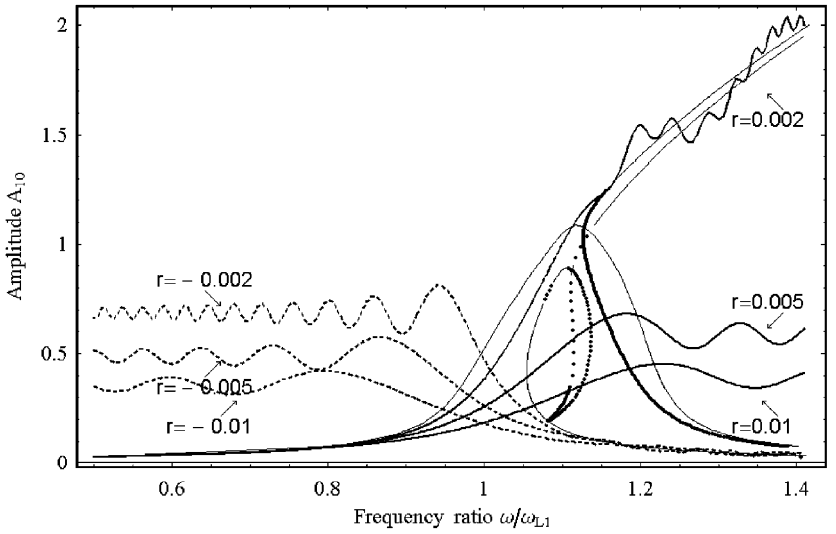

Fig. 10. Passage through fundamental resonance of an undamped clamped-hinged beam at greater rates of changing σ: the course of amplitude is A_{10}.

greater rates of changing σ (compare Figs. 6 and 10). Non-stationary frequency response with decreasing frequency in Figs. 9 and 10 emanates from the lowest part of branch $A_{10}^{\text{in}(3)}$ of the stationary resonance curve. Evidently, there is an important distinction in the passage through fundamental resonance with decreasing frequency, where the beat phenomenon does not die away by approaching towards the stationary resonance curve.

This behavior can be explained through the absence of damping. Due to the nonlinearity again the asymmetry appears between response curves at increasing and decreasing frequencies, respectively.

Figs. 11 and 12 show the passage through fundamental resonance of the second mode oscillation. In Fig. 11, the passage with increasing excitation frequency is conducted by applying the smallest rate of changing σ ($r = 0.0005$) and for decreasing frequency the corresponding negative value of rate is applied. In Fig. 12 the passages at greater rates $r = \pm 0.002$, ± 0.005 and ± 0.01 are considered. Non-stationary frequency responses

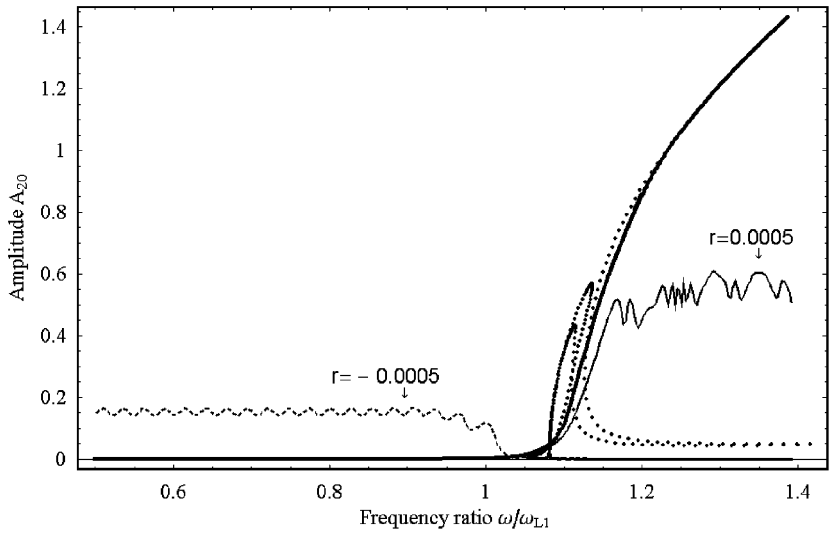

Fig. 11. Passage through fundamental resonance of an undamped clamped-hinged beam at small rates of changing σ: the course of amplitude A_{20}.

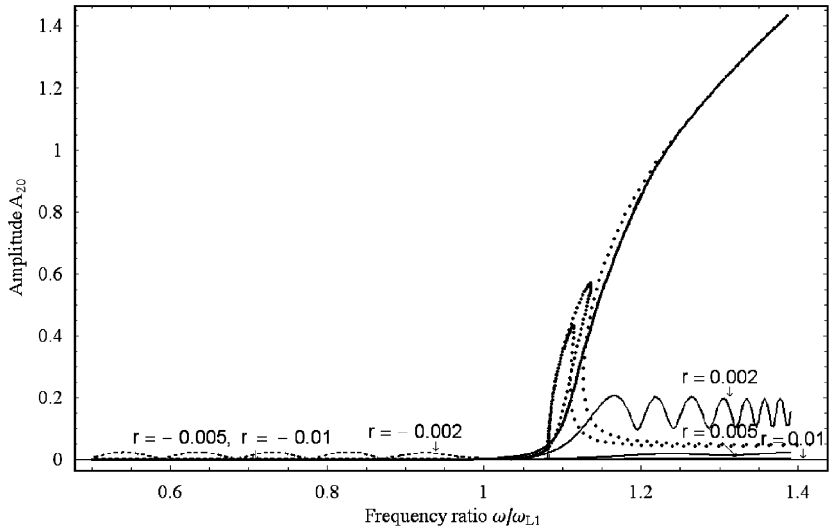

Fig. 12. Passage through fundamental resonance of an undamped clamped-hinged beam at greater rates of changing σ: the course of amplitude A_{20}.

with decreasing frequency in Figs. 11 and 12 emanate from branch $A_{20}^{\mathrm{out}(1)}$ of the stationary curve, which spreads in the vicinity of the frequency axis. The evolution of beat phenomenon obeys the same rules as holds for the first mode oscillation.

Again, the important difference is that the second mode non-stationary oscillation is more weakly excited than the first mode non-stationary oscillation.

6.3. Non-stationary response curves of a clamped-hinged beam depending on varying excitation amplitude

Non-stationary responses of clamped-hinged beam depending on varying excitation amplitude are again governed by Eqs. (50)–(53), where excitation frequency $\omega = \omega_1$, detuning $\sigma = (\omega_0 - \omega_{10})/\varepsilon$ and frequency

$\omega_{21} = (3\omega_1 - \omega_{20})/\varepsilon$ are kept constant and amplitude p_{11} varies slowly with time. In special case of linear time dependence, p_{11} takes the form:

$$p_{11} = p_{11}(0) + r\tau_3, \tag{72}$$

where $p_{11}(0)$ denotes the value of variable excitation amplitude at the starting time and r denotes the rate of changing excitation amplitude. If the excitation frequency ω is less than or equal to the first natural frequency ω_{L_1}, then stationary response amplitudes A_{10} and A_{20} are single-valued and non-stationary responses coincide with stationary ones. This behavior is depicted in Fig. 13 for the value of frequency ratio $\omega/\omega_{L_1} = 0.9$ and damping coefficients $c_1 = c_2 = 0.006$. Note, that oscillations of the second mode are entirely suppressed in both stationary and non-stationary responses (amplitude A_{20} takes zero value at each excitation amplitude p_{11}). If the excitation frequency lies in the range $\omega > \omega_{L_1}$, then the stationary responses of amplitudes A_{10} and A_{20} possess jump phenomenon and loops. At higher values ω, loops disappear. Due to the

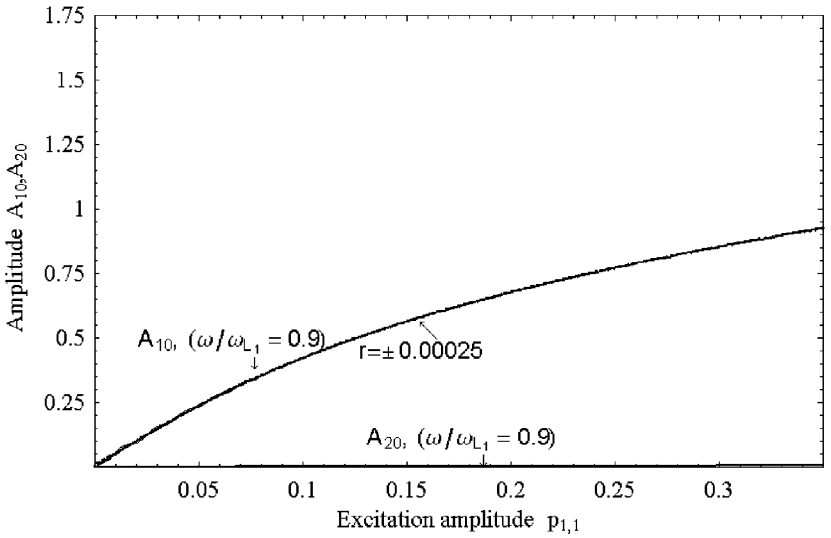

Fig. 13. Stationary and non-stationary responses of amplitudes A_{10} and A_{20} depending on slowly varied excitation amplitude p_{11} at excitation frequency $\omega = 0.9\omega_{L_1}$.

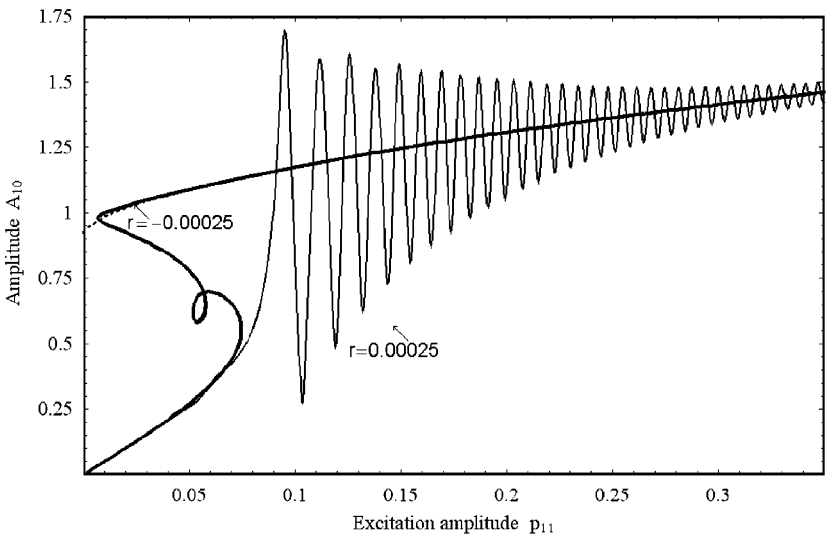

Fig. 14. Stationary and non-stationary responses of amplitude A_{10} depending on slowly varying excitation amplitude p_{11} at excitation frequency $\omega = 1.1\omega_{L_1}$.

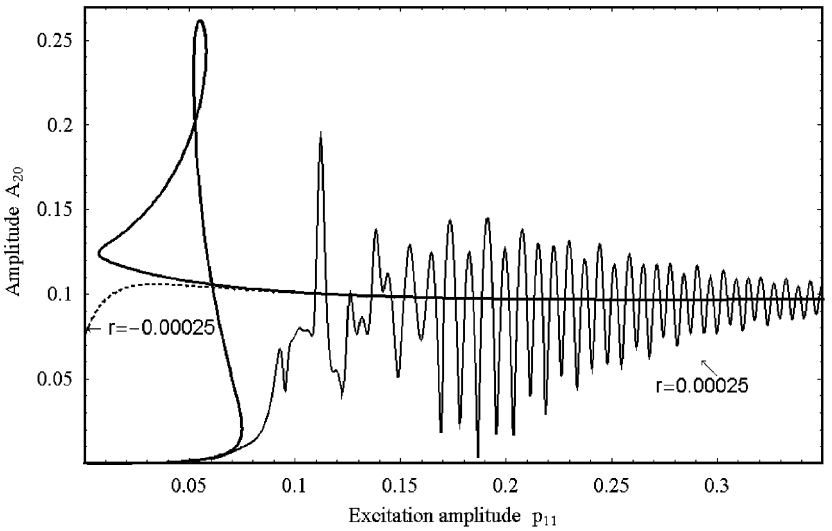

Fig. 15. Stationary and non-stationary responses of amplitude A_{20} depending on slowly varying excitation amplitude p_{11} at excitation frequency $\omega = 1.1\omega_{L_1}$.

jump phenomenon, non-stationary responses of amplitudes A_{10} and A_{20} gradually evolve in the beat phenomenon, which entirely distinguishes from the stationary response. As an example, non-stationary response curves for increasing as well as decreasing excitation amplitude p_{11} are computed for values of frequency ratio $\omega/\omega_{L_1} = 1.1$ and damping coefficients $c_1 = c_2 = 0.006$. Increasing excitation amplitude p_{11} starts with initial value $p_{11}(0) = 0$ and is slowly varied with rate $r = 0.00025$. Decreasing amplitude p_{11} starts with the maximal value of excitation amplitude reached in stationary response and then is slowly varied with rate $r = -0.00025$. Non-stationary response together with corresponding stationary response of amplitude A_{10} is shown in Fig. 14.

When the excitation amplitude p_{11} increases, non-stationary response initially follows the lower stable branch of the stationary curve; however, in the vicinity of the turning point, it leaves the stationary curve and develops a beating phenomenon. At decreasing excitation amplitude, non-stationary response initially follows the upper stable branch of stationary curve and in the vicinity of the turning point leaves the stationary curve approaching the zero-valued amplitude A_{10}. Note that the stationary response indicates a jump phenomenon and a loop is clearly visible in Fig. 14.

The non-stationary response of amplitude A_{20} together with the stationary response is depicted in Fig. 15. Similarly, as in the case of amplitude A_{10}, excitation amplitude p_{11} is firstly increased, where the non-stationary response at the beginning follows the stationary curve and then deviates from it by developing the beat phenomenon. In the passage with decreasing excitation amplitude, non-stationary response first follows the stationary curve and then deviates from it by approaching towards the zero value of amplitude A_{20}.

7. Conclusions

A perturbation method with multiple time scales is presented for N-dof dynamical systems having cubic nonlinearities and is capable of treating non-stationary oscillations, produced by slowly varying parameters. The impact of slowly varying parameters on a system response is considered by adding an additional, slow time scale to the time scales of the nonlinear system, which generally correspond to the incommensurate nonlinear frequencies of the aperiodic response. The method is formulated for studying the non-stationary fundamental, superharmonic and subharmonic resonances under the influence of slowly varying excitation frequency and excitation amplitude, respectively. The non-stationary fundamental resonance of damped as well as undamped clamped-hinged beams by considering internal resonance and by including stability analysis of stationary response is presented in details. Computed non-stationary responses differ very much from

stationary responses. From analysis of non-stationary resonances it can be concluded that the present method offers better insight into the phenomenon of clamped-hinged beam vibrations and cannot be approximated by stationary analysis in the presence of slowly varying parameters. Indeed, responses of stationary resonances are also computed by the present method and results are compared by the IHB method to show good agreement. Branch tracing of the stationary solutions by arc-length continuation is implemented, which leads to the conclusion that the EL–P method is reliable and efficient. Quite so, in the presence of weak nonlinearities, the EL–P method has an evident advantage over the IHB method due to its deficiency of computing non-stationary responses. The EL–P method can be easily generalized for treating dynamical systems with other types of nonlinearities, such as quadratic nonlinearities, as well as treating non-stationary combination resonance, which is beyond the scope of the conventional Lindstedt–Poincare method [11,12].

Acknowledgements

This work has been supported by Grant no. P2-0137-RO-0795 of the Slovenian Ministry of Higher Education, Science and Technology. The author is grateful to the anonymous JSV reviewers and to the editor for their valuable comments that have certainly improved the paper.

References

[1] Y.A. Mitropolski, *Problems of the Asymptotic Theory of Nonstationary Vibrations*, Daniel Davey, New York, 1965.
[2] B.J. Agrawal, R.M. Ewan-Iwanowski, Resonances in nonstationary, nonlinear, multi-degree-of-freedom systems, *AIAA Journal* 11 (7) (1973) 907–912.
[3] A.H. Nayfeh, *Perturbation Methods*, Wiley, New York, 1973.
[4] A.H. Nayfeh, D.T. Mook, *Nonlinear Oscillations*, Wiley, New York, 1979.
[5] S.L. Lau, Y.K. Cheung, S.H. Chen, Alternative perturbation procedure of multiple scales for nonlinear dynamics systems, *ASME Journal of Applied Mechanics* 56 (1989) 667–675.
[6] S.H. Chen, Y.K. Cheung, S.L. Lau, On the internal resonance of multi-degree-of-freedom systems with cubic nonlinearity, *Journal of Sound and Vibration* 128 (1989) 13–24.
[7] S.H. Chen, J.L. Huang, K.Y. Sze, Multidimensional Lindstedt–Poincare method for nonlinear vibration of axially moving beams, *Journal of Sound and Vibration* 306 (1–2) (2007) 1–11.
[8] R.R. Pušenjak, J. Avsec, M.M. Oblak, Extended Lindstedt–Poincare method with multiple time scales for nonstationary oscillations, *Proceedings of the IMECE2006, ASME International Mechanical Congress and Exposition*, Chicago, IL, USA, November 5–10, 2006.
[9] R.R. Pušenjak, M.M. Oblak, Incremental harmonic balance method with multiple time variables for dynamical systems with cubic non-linearities, *International Journal for Numerical Methods in Engineering* 59 (2) (2004) 255–292.
[10] S.H. Chen, Y.K. Cheung, A modified Lindstedt–Poincare method for a strongly non-linear two-degree-of-freedom system, *Journal of Sound and Vibration* 193 (4) (1996) 751–762.
[11] L. Meirovitch, *Fundamentals of Vibrations*, McGraw-Hill, Boston, 2001.
[12] C. Hayashi, *Nonlinear Oscillations in Physical Systems*, Mc-Graw-Hill, New York, 1964.